Nonclassical rotational inertia fraction in a one-dimensional model of a supersolid

Néstor Sepúlveda,[1] Christophe Josserand,[2,3] and Sergio Rica[1]
[1]*Laboratoire de Physique Statistique de l'Ecole Normale Supérieure, 24 Rue Lhomond, 75231 Paris Cedex 05, France*
[2]*Institut Jean Le Rond D'Alembert, UMR 7190 CNRS-UPMC, 4 place Jussieu, 75005 Paris, France*
[3]*Kavli Institute for Theoretical Physics, University of California, Santa Barbara, California 93106, USA*
(Received 26 December 2007; published 25 February 2008)

We study the rotational inertia of a model of supersolid in the frame of the mean field Gross-Pitaevskii theory in one space dimension. We discuss the ground state of the model and the existence of a nonclassical inertia under rotation that models an annular geometry. An explicit formula for the nonclassical rotational inertia (NCRI) is deduced. It depends on the density profile of the ground state, in full agreement with former theories. We compare the NCRI computed through this theory with direct numerical simulations of rotating one-dimensional systems.

DOI: 10.1103/PhysRevB.77.054513 PACS number(s): 67.80.−s

I. INTRODUCTION

Since pioneering works by Andreev and Lifshitz,[1] Chester,[2] Leggett,[3] and others, supersolids have been thought of as a kind of Bose-Einstein condensation of defects, vacancies, or interstitials. They would achieve a coherent state that could allow a matter to flow through the crystal. Although the quest for a supersolid state over the past 40 years has failed,[4] the context has totally changed with the recent experiments by Kim and Chan.[5–7] In these experiments, solid helium[4] fills a torsional oscillator under small oscillations and the rotational frequency is measured. Surprisingly, the rotational inertia shows a drop at temperatures below a few tenths of Kelvin. This nonclassical rotational inertia (NCRI) is believed to be the signature of the transition of a fraction of the solid into a supersolid state. The situation has become puzzling as other experiments have been performed. Thus, although the drop of the moment of inertia has been confirmed, crystal annealing was shown to lower dramatically the amplitude of this NCRI.[8,9] Similarly, solid helium submitted to pressure gradient could not flow except when large grain boundaries were present in the sample.[10–12] Moreover, the responses of solid ^{4}He to a localized pressure jump presented no evidence of superflow in the solid.[13,14] The experimental context thus presents apparent contradictions between NCRI measurements and pressure driven flows with the role of disorder (through vacancies, grain boundaries, etc.) to be elucidated. On the other hand, the theoretical framework for describing supersolids also presents some fundamental puzzles (see the recent review of Prokof'ev,[15] where the influence of the disorder is particularly discussed). Besides the argument of Penrose and Onsager,[16] Monte Carlo models claim that a perfect crystal cannot exhibit supersolid behavior.[17,18] However, the account for exchange processes between neighboring atoms,[3,19] the densities, and the role of the vacancies in the dynamics raise additional fundamental questions on the existence and the nature of the supersolidity (see Refs. 20 and 21, for instance).

An alternative issue consists of using the Gross-Pitaevskii (GP) model[22] to describe the dynamics of a quantum solid, as proposed in 1994 by Pomeau and Rica.[23] The original GP equation[22] is used, with a roton minimum in the dispersion relation, where the ground state exhibits a first order phase transition to a crystalline state. However, the assumptions underlying the GP equation are not, strictly speaking, valid for helium although this equation is believed to give a good qualitative description of superfluid helium. Therefore, this model, even crude in its basic structure, is at least a good test bed for theories of supersolids that are still in a state of uncertainty. In Refs. 24 and 25, Josserand *et al.* have developed the theory for the long wave perturbations of this model of supersolid and have shown that this model was able to conciliate the apparent experimental contradiction discussed above. In the present paper, we study the one-dimensional (1D) version of this model. Besides the simplicity of the 1D approach, which then allows precise determination of the crystal structure, the 1D limit is particularly interesting since it can model an annular geometry to some extent.

II. MODEL

The starting point is the original GP equation[22] for the complex wave function $\psi(x,t)$ in one space dimension:

$$i\hbar\frac{\partial\psi}{\partial t} = -\frac{\hbar^2}{2m}\frac{\partial^2\psi}{\partial x^2} + \psi\int_{-\infty}^{\infty} U(|x-y|)|\psi(y)|^2 dy, \qquad (1)$$

where $U(s)$ is the two body potential depending on the relative distance. The potential $U(s)$ should satisfy

$$0 < \int_{-\infty}^{\infty} U(s)ds < \infty$$

for stability of the long wave modes [see the dispersion relation in Eq. (4) below]. The Fourier transform

$$\hat{U}_k = \int_{-\infty}^{\infty} U(s)e^{iks}ds \qquad (2)$$

has to be bounded for all k; moreover, as we will see later, we shall also require that the Fourier transform $\hat{U}_k$ become negative at some wave number to allow roton crystallization.

This dynamics is Hamiltonian,

$$i\hbar\partial_t\psi = \frac{\delta H}{\delta\psi^*},$$

and the energy or Hamiltonian

$$H = \frac{\hbar^2}{2m}\int_{-\infty}^{\infty}|\partial_x\psi|^2dx + \frac{1}{2}\int_{-\infty}^{\infty}\int_{-\infty}^{\infty}U(|x-y|) \times|\psi(y)|^2|\psi(x)|^2dydx, \quad (3)$$

as well as the number of particles

$$N = \int_{-\infty}^{\infty}|\psi(x)|^2dx$$

and the linear momentum

$$P = -\frac{i\hbar}{2}\int_{-\infty}^{\infty}(\psi^*\partial_x\psi - \psi\partial_x\psi^*)dx,$$

is conserved. According to the energy, the ground-state solution is real since any nonuniform phase increases its energy.

The dynamics indeed exhibits a homogeneous and stationary solution $\psi_0=\sqrt{n_0}e^{-i(E_0/\hbar)t}$, with n_0 the mean 1D density and $E_0=n_0\int_{-\infty}^{\infty}U(s)ds$. This solution is stable and can also be the ground state for small enough n_0, as suggested by the Bogoliubov spectrum of the perturbations[26] (see below):

$$\hbar\omega_k = \sqrt{(\hbar^2k^2/2m)^2 + (\hbar^2k^2/m)n_0\hat{U}_k}. \quad (4)$$

Assuming that the potential scales like U_0 and possesses a single length scale a, the spectrum then depends only on a single dimensionless parameter:[23]

$$\Lambda = n_0\frac{ma^2}{\hbar^2}\hat{U}_0,$$

with $\hat{U}_0=\int_{-\infty}^{\infty}U(s)ds=2aU_0$. For some analytical results and for the numerics later on, we choose the soft core interaction, with no loss of generalities:

$$U(|x-y|) = U_0\theta(a-|x-y|), \quad (5)$$

with $\theta(\cdot)$ the Heaviside function. The Fourier transform of this special interaction potential is

$$\hat{U}_k = 2U_0\frac{\sin(ka)}{k} = \hat{U}_0\frac{\sin(ka)}{ka}.$$

It should also be noticed that the special choice of the potential in Eq. (5) is purely of practical interest because it is easy to implement in some numerical schemes and can be easily used for variational estimates. Other functions whose Fourier transform would be negative for a wave-number domain (strictly bigger than zero) would show similar properties. Among them are the classical two body atomic potential with strong repulsion at short scale and a slight attraction for large scale or a potential $\hat{U}_k$ chosen in such a way that the Bogoliubov dispersion relation matches the Landau spectrum with the right values of the speed of sound c and the three roton parameters.[27]

With $x'=x/a$, $t'=\frac{\hbar}{ma^2}t$, and $\psi'=\psi/\sqrt{n_0}$, the dimensionless GP equation for the Heaviside interaction (we drop the primes hereafter) reads

$$i\frac{\partial\psi}{\partial t} = -\frac{1}{2}\frac{\partial^2\psi}{\partial x^2} + \frac{\Lambda}{2}\psi(x,t)\int_{x-1}^{x+1}|\psi(y)|^2dy. \quad (6)$$

Finally, we emphasize that an annular geometry can be simplified into a 1D system by considering the periodic boundary condition $\psi(x,t)=\psi(x+L,t)$ (L is dimensionless) and by assuming that the transverse structure of the solid can be neglected. We then define the energy and number of particles densities:

$$\mathcal{E} = \frac{1}{2L}\int_0^L\left(|\psi_x|^2 + \frac{\Lambda}{2}|\psi|^2\int_{x-1}^{x+1}|\psi(y)|^2dy\right)dx, \quad (7)$$

$$1 = \frac{1}{L}\int_0^L|\psi(x,t)|^2dx. \quad (8)$$

III. GROUND STATE

As shown in Ref. 23, for low Λ, the ground state is a superfluid (without positional order). However, above a critical value, Λ_c, the ground state shows a periodic modulation of the density in space. Although the transition is first order as Λ increases in two and three space dimensions, it is supercritical (second order) in one space dimension.[31] The periodic structure arising from the instability can be analytically estimated through a variational approach for a fixed wavelength λ at least in two regimes: close to the transition and for large Λ.

If $\Lambda \gtrsim \Lambda_c$, a weak amplitude development of wave number k and normalized to unity reads

$$\psi(x) = \frac{1}{\sqrt{1+2|A|^2}}(1 + Ae^{ikx} + A^*e^{-ikx}). \quad (9)$$

Minimizing the energy of such solution gives

$$|A|^2 = -\frac{k^2 + 4\Lambda\hat{U}_k/\hat{U}_0}{2[k^2 + \Lambda(\hat{U}_{2k} - 4\hat{U}_k)/\hat{U}_0]} \quad (10)$$

and the wave-number selection $k_ca=4.078\cdots$. The amplitude for this wave number k_c follows

$$|A|^2 = \frac{-8\sin(k_c)}{k_c^3[8-\cos(k_c)]}(\Lambda-\Lambda_c) \approx 0.011(\Lambda-\Lambda_c).$$

In the large Λ limit, the density exhibits strongly nonlinear structures since the potential energy in Eq. (7) requires ψ to be very small while the mass normalization in Eq. (8) forbids ψ everywhere. Therefore, the energy minimization leads to a periodic structure with zones where $\psi\approx 0$ and zones where $\psi \gg 1$. In the $\Lambda\to\infty$ limit, Ref. 28 showed that $\psi\neq 0$ only in a small zone $x\in(-\delta,\delta)$ of the whole period $(0,\lambda)$. The Euler-Lagrange condition deduced from Eq. (7) together with Eq. (8) leads to the Helmholtz equation in the

domain $(-\delta,\delta):-\psi''(x)=\mu\psi$. Finally, the minimization of the energy gives δ and the wave number λ of the periodic structure. Following this approach, we now sketch an estimate of the ground state for finite $\Lambda \gg 1$. We use the trial function for a single period:

$$\psi(x) = \sqrt{\frac{\lambda}{\delta}}\cos\left(\frac{\pi x}{2\delta}\right) \tag{11}$$

in $x \in [-\delta,\delta]$ and zero elsewhere, that satisfies exactly the normalization condition in Eq. (8). By introducing this trial function into the energy in Eq. (7), we obtain $\mathcal{E}=\mathcal{E}_1+\mathcal{E}_2+\mathcal{E}_3$, with the kinetic energy

$$\mathcal{E}_1 = \frac{\pi^2}{8\delta^2},$$

the self-interaction of a pulse with itself,

$$\mathcal{E}_2 = \frac{\Lambda\lambda}{4},$$

and the nontrivial interaction of a pulse with its two near neighbors,

$$\mathcal{E}_3 = \frac{\Lambda}{2}\int_{\lambda-1-\delta}^{\delta}\psi(x)^2\int_{-\delta}^{x+1-\lambda}\psi(y)^2 dy dx.$$

This energy $\mathcal{E}_3$ is not zero only if $\lambda < 1+2\delta$ (and naturally, we have $\lambda > 2\delta$).

The energy $\mathcal{E}$ may be understood as a function of δ and of the periodicity length λ. Then, the variation of total energy in the (δ,λ) plane shows the existence of a global minimum and a saddle for large enough Λ. As Λ decreases, the saddle and the global minimum collide, and we obtain a pure monotonic energy landscape in the (δ,λ) plane, leading to both λ and δ to infinity as minimizer. On the other hand, when $\Lambda\to\infty$, the global minimum moves to $(\delta,\lambda)\to(0,1)$. This selection mechanism holds for an infinite domain where the wavelength λ can vary continuously. In a finite domain, λ can only take discrete values related to the number N_c of unitary cells, $\lambda = L/N_c$. Numerical simulations also suggest the existence of a large energy barrier between minimizers with different numbers of cells, N_c, for large Λ. Thus, for a given domain size L, the energy as a function of (δ,λ) is now described by a discrete set of energy functions of δ for each available λ satisfying $\lambda = L/N_c$. One now has to minimize each energy with respect to δ. For small Λ (typically smaller than Λ_c), none of these functions have minima. For large Λ on the other hand, there is a finite band of λ for which the energy admits a minimum as δ varies. The minimization of this energy with respect to δ provides relations among δ and Λ with the wavelength λ as a fixed parameter. To determine the global minimum and to avoid further algebraic difficulties, we introduce the new variable $z = \pi(\lambda-1)/\delta$, where $0 \leqslant z \leqslant 2\pi$ for our problem (in particular, $z > 2\pi$ means that the peaks do not interact with one another). Minimizing the energy gives the following relation for $\Lambda = \Lambda(\lambda, z)$:

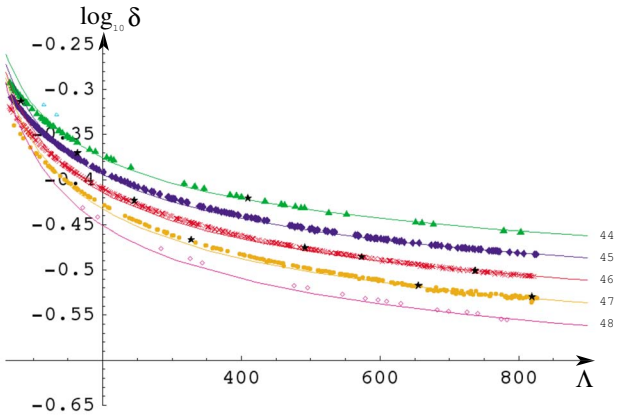

FIG. 1. (Color online) Plot of $\log_{10}\delta$ as a function of Λ for different λ. The curves correspond to formula (12) while the points come from numerical simulations. The total size of the system is 64 units and the range of the interaction is $a=16$. The system displays a number of cells varying from 44 to 48 (identified at the right hand side of the figure). The respective λ thus vary from 4/3 to 16/11.

$$\Lambda = \frac{4\pi^2 z}{\lambda(\lambda-1)^2\{(2\pi-z)[\cos(z)+2]+3\sin(z)\}}. \tag{12}$$

Figure 1 shows δ versus Λ for different values of λ. The analytical curves are shown together with the results of direct numerical simulations described below.

Finally, an exponential "boundary layer" correction develops near $x=\pm\delta$ where the nonlinear term in Eq. (6) cannot be neglected, as noticed by Ref. 28. In the limit of large Λ, where, similarly, $\lambda\to 1$, the nonlinear term of Eq. (6) gives the following near $x=\delta$:

$$\lim_{\lambda\to 1}\int_{x-1}^{x+1}\psi(y)^2 dx = Cte + \lim_{\lambda\to 1}\int_{\lambda-\delta}^{x+1}\psi(y)^2 dx$$

$$\approx Cte + \frac{\pi^2}{12\delta^3}(x-\delta)^3 + \mathcal{O}[(x-\delta)^4].$$

The ground state is thus modified into $\psi(x)+\varphi(x)$, where $\psi(x)$ is the trial function in Eq. (11), and φ satisfies a linear Schrödinger equation:

$$-\frac{1}{2}\varphi''(x) + \frac{\Lambda}{2}V(x)\varphi(x) = 0,$$

where the first nontrivial term, for the potential reads $V(x) = \frac{\pi^2\lambda}{12\delta^3}(x-\delta)^3$. The solution may be computed directly in terms of Bessel functions: $\varphi(x) = K_*\sqrt{x}K_{1/5}\left[\frac{\pi}{5}\sqrt{\frac{\Lambda\lambda}{3\delta^3}}(x-\delta)^{5/2}\right]$, where the constant K_* results from the matching of the exponentially small boundary layer and the trial function. One can also expand this solution via a WKB approximation: $\varphi(x) = K_* e^{-\sqrt{\Lambda}S(x)}$ with $S(x) = S_0(x) + \frac{1}{\sqrt{\Lambda}}S_1(x) + \cdots$. We then obtain $S_0(x) = \int\sqrt{V(x)}dx$ and $S_1(x) = \frac{1}{2}\log[S_0'(x)]$ and, therefore,

$$\varphi(x) = \frac{K_*}{\sqrt{S_0'(x)}}e^{-\sqrt{\Lambda}S_0(x)},$$

with $S_0(x) = \frac{\pi\sqrt{\lambda/3}}{5\delta^{3/2}}(x-\delta)^{5/2}$.

IV. NONCLASSICAL MOMENT OF INERTIA IN SUPERFLUIDS AND SUPERSOLIDS

The precise estimation of the ground state is in fact crucial in describing the supersolid features of the model. Indeed, we have obtained in Refs. 24 and 25, using the homogenization technique,[29] an expression for the effective or superfluid density matrix ϱ_{ik}^{ss} deduced from the density profile of the crystal. We shall in fact explore the low excited states around the ground state, described by the knowledge of the crystal density $\rho_0(x)$. The change of energy for phase variations gives

$$\Delta E = \frac{1}{2}\int \rho_0(x)\left(\frac{\partial \phi}{\partial x}\right)^2 dx \tag{13}$$

and ϕ is determined by minimizing ΔE, which corresponds to the Euler-Lagrange condition

$$\frac{\partial}{\partial x}\left(\rho_0(x)\frac{\partial \phi}{\partial x}\right) = 0 \tag{14}$$

under the appropriate boundary conditions. As shown by Leggett,[3] for a periodic $\rho_0(x)$ under rotation, ΔE is lower than that of a rigid solid rotation, which indicates that superfluidity is present.

In Refs. 24 and 25, we have obtained an expression for the energy variation in three space dimensions: $\Delta E = \frac{\hbar^2}{2m}\int \varrho_{ik}^{ss}\partial_i\phi\partial_k\phi d\boldsymbol{r}$, where ϱ_{ik}^{ss} is the effective or superfluid density matrix. It can be explicitly expressed using a solution of a partial differential equation in the unit cell V of the solid following

$$\varrho_{ik}^{ss} = n\delta_{ik} - \frac{1}{V}\int_V \rho_0(\boldsymbol{r})\,\boldsymbol{\nabla} K_i \cdot \boldsymbol{\nabla} K_k d\boldsymbol{r}. \tag{15}$$

The vector K_i is a periodic function in the unit cell V that is a solution of $\nabla_i\rho_0 + \boldsymbol{\nabla}\cdot(\rho_0\boldsymbol{\nabla}K_i) = 0$.

A. Nonclassical rotational inertia in one space dimension

In one space dimension, we can in fact deduce the density ϱ^{ss} exactly. Indeed formula (15) simplifies then into one term:

$$\varrho^{ss} = n - \frac{1}{\lambda}\int_0^\lambda \rho_0(x)(\partial_x K_x)^2 dx,$$

where $K_x(x)$ is a periodic function in the interval $[0,\lambda]$ solution of $\partial_x\rho_0 + \partial_x(\rho_0\partial_x K_x) = 0$. Thus, $\partial_x K_x(x) = -1 + \frac{c}{\rho_0(x)}$, where c is an integration constant. The periodic boundary condition $K_x(0) = K_x(\lambda)$ gives

$$c = \frac{1}{\frac{1}{\lambda}\int_0^\lambda \frac{1}{\rho_0(x)}dx}.$$

Finally, we find that in one dimension, the superfluid density writes

$$\frac{1}{\varrho_{ss}} = \frac{1}{c} = \frac{1}{\lambda}\int_0^\lambda \frac{1}{\rho_0(x)}dx.$$

Thus, the theory of homogenization provides us an exact result for the special case of one space dimension, and the effective density (scalar in one dimension) is then a kind of "harmonic" average of the density.[29] From this formula, the nonclassical rotational inertia fraction (NCRIF) ϱ^{ss}/ρ corresponds exactly to the upper bound quotient Q_0 proposed by Leggett,[3] who also established the equivalence for 1D systems more recently.[30] Therefore, the NCRIF at low speed (NCRIF_0) reads

$$\varrho^{ss}/\rho = Q_0 \equiv \frac{1}{\left[\frac{1}{\lambda}\int_0^\lambda \rho_0(x)dx\right]\left(\frac{1}{\lambda}\int_0^\lambda \frac{1}{\rho_0(x)}dx\right)}. \tag{16}$$

The following remarks can be made:

(1) The Schwartz inequality[32] and $\rho_0(x) \geqslant 0$ give $0 \leqslant Q_0 \leqslant 1$.

(2) If the ground state of finite energy vanishes at some point, then the nonclassical rotational inertia does as well. Indeed, if at some point $x*$ we have $\rho_0(x) \sim |x - x*|^\alpha$ with $\alpha > 0$, then

$$\int_0^\lambda \frac{1}{\rho_0(x)}dx \approx (\text{finite term}) + \int_{x*-\epsilon}^{x*+\epsilon} |x - x*|^{-\alpha}dx$$

and

$$Q_0 \approx \frac{1}{(\text{finite term}) + \frac{2}{1-\alpha}\epsilon^{1-\alpha}}.$$

Therefore, if $0 < \alpha \leqslant 1$, Q_0 remains finite with $\epsilon \to 0$. However, such a ground state would require an infinite amount of energy. Indeed, if the ground state vanishes at some point $x*$ as $\psi_0(x) \sim |x - x*|^{\alpha/2}$ with $0 < \alpha \leqslant 1$, then it requires an infinite energy because the energy in Eq. (3) diverges as

$$\int \psi_0'(x)^2 dx \approx (\text{finite term}) + \alpha^2\int_{x*-\epsilon}^{x*+\epsilon} |x - x*|^{\alpha-2}dx$$

$$\approx (\text{finite term}) + \mathcal{O}(\epsilon^{\alpha-1})$$

when $\epsilon \to 0$.

B. Nonclassical rotational inertia fraction in the weakly nonlinear limit

The NCRIF in the limit of weak modulation may be computed directly from the trial function in Eq. (9):

$$Q_0 = \frac{(1 - 4|A|^2)^{3/2}}{(1 + 2|A|^2)}, \tag{17}$$

where $|A|^2$ is evaluated at $k = k_c$. As $|A| \to 1/2$, the quotient Q_0 vanishes because the wave function in Eq. (9) vanishes at some point.

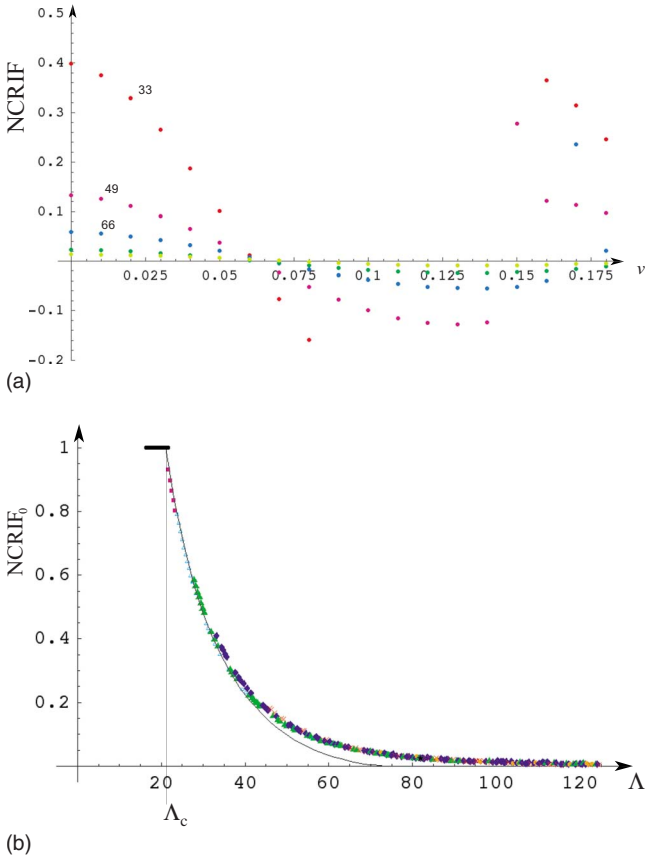

FIG. 2. (Color online) (a) NCRIF as a function of v for different values of Λ. (b) NCRIF_0 as a function of Λ; the line is the curve from the weakly nonlinear analysis, see formula (17) which gives a good approximation up to $\Lambda \approx 40$.

C. Nonclassical rotational inertia fraction in the limit $\Lambda \to \infty$

For large Λ, since the ground state $\rho_0(x)$ decays exponentially, the contribution to the NCRIF in Eq. (16) mainly comes from the large contribution of $1/\rho_0(x)$ in $x \in [\delta, \lambda/2]$. That is, after using the WKB approximation:

$$Q_0 \approx \frac{5}{4} K_*^2 e^{-\pi/5\sqrt{\Lambda\lambda/3\delta^3}(\lambda/2-\delta)^{5/2}}. \tag{18}$$

V. RESULTS

We will now be using numerical simulations to deduce the NCRI and compare it with theories by two different methods. First, the ground state is determined. Then, one can compute directly the NCRI by imposing a rotation to this ground state. On the other hand, the value of Q_0 can be calculated from the ground-state solution $\rho_0(x)$.

Numerical results are obtained by minimizing the energy in Eq. (7) under the number of particles condition in Eq. (8). We therefore use the Ginzburg-Landau version of the dynamics which can be interpreted as the integration of the GP equation for imaginary time $t=-i\tau$:

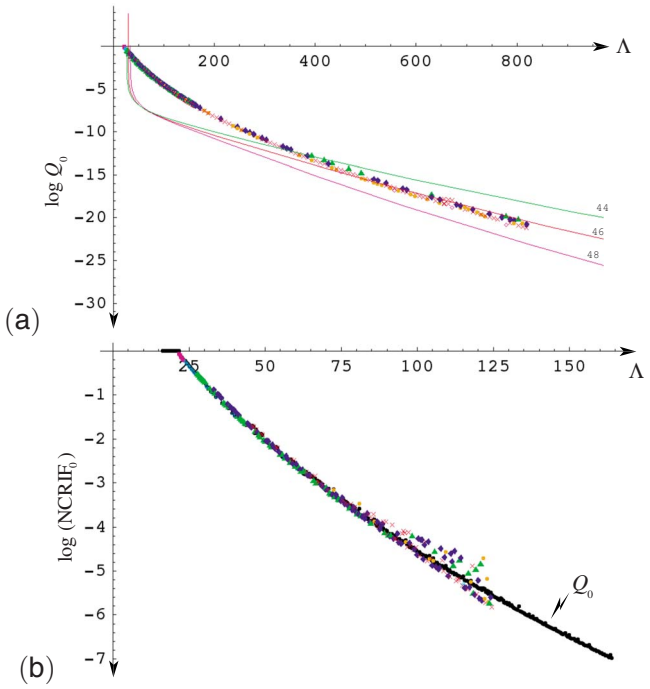

FIG. 3. (Color online) (a) The quotient Q_0 as a function of Λ using a direct numerical integration of ground states $\rho_0(x)$ obtained for Fig. 1. The lines are the functions obtained from the theory in Eq. (18) for three different wavelengths (similar notations as in Fig. 1) with $K_*=0.01$ as a fixed parameter. Notice the exponential behavior in qualitative agreement with Eq. (18). (b) Comparison between the numerical calculations NCRIF_0 and Leggett's quotient Q_0 represented with black dots.

$$\frac{\partial\psi}{\partial\tau} = \mu\psi + \frac{1}{2}\frac{\partial^2\psi}{\partial x^2} - \frac{\Lambda}{2}\psi(x,t)\int_{x-1}^{x+1}|\psi(y)|^2 dy. \tag{19}$$

μ is the Lagrangian multiplier introduced to satisfy the number of particles condition.

Imposing a rotational frequency ω in a 1D annular system amounts to considering a drift of the system at constant velocity $v=\omega L$ with periodic boundary conditions. The ground state of such a system is obtained by minimizing $\mathcal{F}=\mathcal{E}+v\mathcal{P}+\mu(N-n_0)$, where $\mathcal{P}=-\frac{i}{2L}\int_0^L[\psi^*(x)\partial_x\psi(x)-\psi(x)\partial_x\psi^*(x)]dx$. Consequently, a direct computation of the NCRIF can be performed numerically:

$$\mathrm{NCRIF}(v) = 1 - \frac{|\mathcal{P}'(v)|}{\int_0^L |\psi(x)|^2 dx}.$$

Figure 2(a) shows the function NCRIF(v) for different Λ obtained by numerical minimization of $\mathcal{F}$. As expected, the NCRIF decreases as v increases. For large value of the parameter v, the NCRIF first becomes negative and then shows large fluctuations, indicating that complex structures are present, such as 2π phase jumps (similar to vortices in higher dimensions). Moreover, numerical instabilities are

also enhanced by the rotation so that only moderate Λ (up to 150) values could be achieved with full confidence.

The low speed limit:

$$\mathrm{NCRIF}_0 = \lim_{v \to 0} \mathrm{NCRIF}(v),$$

is then shown in Fig. 2(b) as a function of Λ and compared with the analytical quotient in Eq. (17) of the weak amplitude modulations, showing an excellent agreement.

On the other hand, as explained above, the NCRIF_0 can be calculated directly from the numerical solution $\rho_0(x)$ by computing the Leggett quotient Q_0 in Eq. (16). Since the ground-state solution is numerically more stable to obtain than the minimization of the rotating system, we are able to compute a satisfactory good estimate for Q_0 up to Λ of the order of 800, as shown in Fig. 3(a). Remarkably, Q_0 does not depend on the wavelength of the periodic structure λ, since all the numerical data for different λ gather on a single curve. This is a consequence of that the main contribution to the quotient Q_0 comes from the wide region with small values of $\rho_0(x)$. On the other hand, only poor agreement is found with the asymptotic behavior in Eq. (18).

In Fig. 3(b), we compare this quotient Q_0 with the NCRIF_0 obtained by direct numerical simulation of the rotating system for the accessible moderate Λ values. It shows a particularly good numerical agreement between the two methods, as expected by the theory.

VI. CONCLUSION

In conclusion, we have studied a model of supersolid in the context of annular geometry using both direct numerical simulation and analytical estimates on the ground-state solution. The ground-state characteristics, that is, the peak matter size δ, is compared with the findings of the numerics for a broad range of variations of the pertinent dimensionless parameter Λ and for some allowed different wavelengths λ. The agreement is completely satisfactory. Next, we compared the exact nonclassical rotational inertia for a one-dimensional periodic ground state, the Leggett quotient Q_0, with the NCRIF computed from the numerics, showing full agreement. We show that the remarkable property of NRCI scales as $\log \varrho_{ss} \sim -\sqrt{\Lambda}$, which is only a tiny fraction because of the exponentially small dependence of the profile of the ground-state density with Λ.

ACKNOWLEDGMENTS

C.J. acknowledges the financial support of the DGA. This research was supported in part by the National Science Foundation under Grant No. PHY05-51164. S.R. acknowledges Anillo de Investigación Act. 15 (Chile).

[1] A. F. Andreev and I. M. Lifshitz, Sov. Phys. JETP **29**, 1107 (1969).
[2] G. V. Chester, Phys. Rev. A **2**, 256 (1970).
[3] A. J. Leggett, Phys. Rev. Lett. **25**, 1543 (1970).
[4] M. W. Meisel, Physica B **178**, 121 (1992).
[5] E. Kim and M. H. W. Chan, Nature (London) **427**, 225 (2004).
[6] E. Kim and M. H. W. Chan, Science **305**, 1941 (2004).
[7] E. Kim and M. H. W. Chan, Phys. Rev. Lett. **97**, 115302 (2006).
[8] Ann Sophie C. Rittner and J. D. Reppy, Phys. Rev. Lett. **97**, 165301 (2006).
[9] Ann Sophie C. Rittner and J. D. Reppy, Phys. Rev. Lett. **98**, 175302 (2007).
[10] D. S. Greywall, Phys. Rev. B **16**, 1291 (1977).
[11] G. Bonfait, H. Godfrin, and B. Castaing, J. Phys. (Paris) **50**, 1997 (1989).
[12] S. Sasaki, R. Ishiguro, F. Caupin, H. J. Maris, and S. Balibar, Science **313**, 1098 (2006).
[13] J. Day, T. Herman, and J. Beamish, Phys. Rev. Lett. **95**, 035301 (2005).
[14] J. Day and J. Beamish, Phys. Rev. Lett. **96**, 105304 (2006).
[15] N. Prokof'ev, Adv. Phys. **56**, 381 (2007).
[16] O. Penrose and L. Onsager, Phys. Rev. **104**, 576 (1956).
[17] D. M. Ceperley and B. Bernu, Phys. Rev. Lett. **93**, 155303 (2004).
[18] N. Prokof'ev and B. Svistunov, Phys. Rev. Lett. **94**, 155302 (2005).
[19] A. J. Leggett, Science **305**, 1921 (2004).
[20] P. W. Anderson, W. F. Brinkman, and D. A. Huse, Science **310**, 1164 (2005).
[21] D. E. Galli, M. Rossi, and L. Reatto, Phys. Rev. B **71**, 140506(R) (2005).
[22] L. P. Pitaevskiĭ, Sov. Phys. JETP **13**, 451 (1961); E. P. Gross, J. Math. Phys. **4**, 195 (1963).
[23] Y. Pomeau and S. Rica, Phys. Rev. Lett. **72**, 2426 (1994).
[24] C. Josserand, Y. Pomeau, and S. Rica, Phys. Rev. Lett. **98**, 195301 (2007).
[25] C. Josserand, Y. Pomeau, and S. Rica, Eur. Phys. J. Spec. Top. **146**, 47 (2007).
[26] N. N. Bogoliubov, J. Phys. (USSR) **11**, 23 (1947).
[27] L. D. Landau, J. Phys. (USSR) **5**, 71 (1941).
[28] A. Aftalion, X. Blanc, and R. L. Jerrard, Phys. Rev. Lett. **99**, 135301 (2007).
[29] A. Bensoussan, J. L. Lions, and G. Papanicolaou, *Asymptotic Analysis in Periodic Structures* (North-Holland, Amsterdam 1978).
[30] A. J. Leggett, J. Stat. Phys. **93**, 927 (1998).
[31] With the potential constructed in Eq. (5), the critical value is $\Lambda_c = 21.05\cdots$.
[32] This inequality reads $[\int_0^\lambda f(x)^2 dx][\int_0^\lambda g(x)^2 dx] \geqslant [\int_0^\lambda f(x)g(x)dx]^2$.